Supporting Information

# Palladium nanospheres embedded metal–organic frameworks to enhance the ECL efficiency of 2,6-dimethyl-8-(3-carboxyphenyl)4,4'-difluoroboradiazene in aqueous solution for ultrasensitive $Cu^{2+}$ detection

Shu-Shu Song, Jia-Le Zhan, Hao-Tian Zhu, Jing-Yi Bao, Ai-Jun Wang, Pei-Xin Yuan*, Jiu-Ju Feng*

*Key laboratory of the Ministry of Education for Advanced Catalysis Materials, College of Chemistry and Materials Science, College of Geography and Environmental Sciences, Zhejiang Normal University, Jinhua 321004, China*

**Corresponding authors: ypxdr@zjnu.edu.cn (P.X. Yuan); jjfeng@zjnu.cn (J.J. Feng).*

## Experimental

### 1. Reagents and materials

Herein, 2,4-dimethylpyrrole, 4-formylbenzoic acid, acetonitrile (ACN), tetrabutylammonium perchlorate (TBAP), methyl alcohol, trifluoroacetic acid (TFA), dichlorodicyanobenzoquinone (AR), triethylamine (TEA), boron trifluoride diethyl etherate (AR), ethyl acetate (AR), methyl alcohol (AR), palladium chloride ($PdCl_2$), 1,2,4,5-benzenetetramine (BTA), sodium borohydride ($NaBH_4$), aqueous ammonia ($NH_3 \cdot H_2O$), 5,5-dimethyl-1-pyrroline N-oxide (DMPO), 2,2,6,6-tetramethyl-4-piperidinol (TMP), p-benzoquinone, NaOH, $MgSO_4$, and $K_2S_2O_8$ were obtained from Aladdin Biochemical Technology Co., Ltd. (Shanghai, China). Phosphate buffer solution (PBS, pH 7.40, 0.10 M $KH_2PO_4/Na_2HPO_4$) was prepared with ultrapure water, which was obtained from a Millipore water purification system (≥18 MΩ, Milli-Q, Millipore) and used throughout all of the assays.

### 2. Apparatus

The morphology and structure of the samples were characterized by scanning electron microscopy (SEM) with a Hitachi S-4800 scanning electron microanalyzer. Transmission electron microscopy (TEM) and high-resolution transmission electron microscopy (HR-TEM) measurements were taken on a JEM-2100F microscope operating at an acceleration voltage of 200 kV. X-ray photoelectron spectroscopy (XPS) analysis was performed on a Thermo VG ESCALAB 250 spectrometer with an Al Kα X-ray irradiation (1486.6 eV) for excitation operated at 120 W, and the data were calibrated by the binding energy of C 1s. Fluorescence (FL) measurements were

conducted with an RF-6000 spectrometer (Thermo Fisher Scientific, America). ECL plots were taken with a home-made ECL spectroscopy acquiring system (consisting of an Acton SP2300i monochromator) equipped with a liquid $N_2$ cooled PyLoN 400BR-eXcelon digital CCD detector (Princeton Instruments, USA) and a VersaSTAT 3 electrochemical analyzer (Princeton Applied Research, USA). NMR hydrogen spectroscopy ($^1$H-NMR) measurement was conducted with a Bruker AMX-500 spectrometer at 600 MHz (Bruker., Germany), by employing tetramethylsilane (TMS) as the reference and deuterated acetone ($C_3D_6O$) as the solvent. The sample compositions were examined by liquid chromatography/mass spectrometry (LC/MS, 6230 TOF, Agilent Technologine Co., Ltd., USA) with the mobile phase (mainly containing methanol and water). Electron paramagnetic resonance (EPR) measurements were conducted on a Bruker EPR EMX plus -9.5/12 by applying a continuous excited potential of 1.50 V.

A classical three-electrode system was used in the electrochemical experiments, in which a glassy carbon electrode (GCE, $\Phi$ = 5mm) acted as the working electrode, an Ag/AgCl electrode (saturated KCl) as the reference electrode and a platinum wire as the counter electrode. Electrochemistry and ECL experiments were performed at CHI 660D electrochemical workstation (Chenhua Analytical Instrument Co., Ltd., China) and MPI-E multi-function ECL analyzer (Xi'an Remax Analytical Instrument Co., Ltd., China), respectively. Electrochemical impedance spectra (EIS) were recorded in a 0.1 M KCl solution containing 5 mM $K_3[Fe(CN)_6]/K_4[Fe(CN)_6]$ by using an alternating voltage of 10 mV in a frequency range of 0.1 ~ 100,000 Hz.

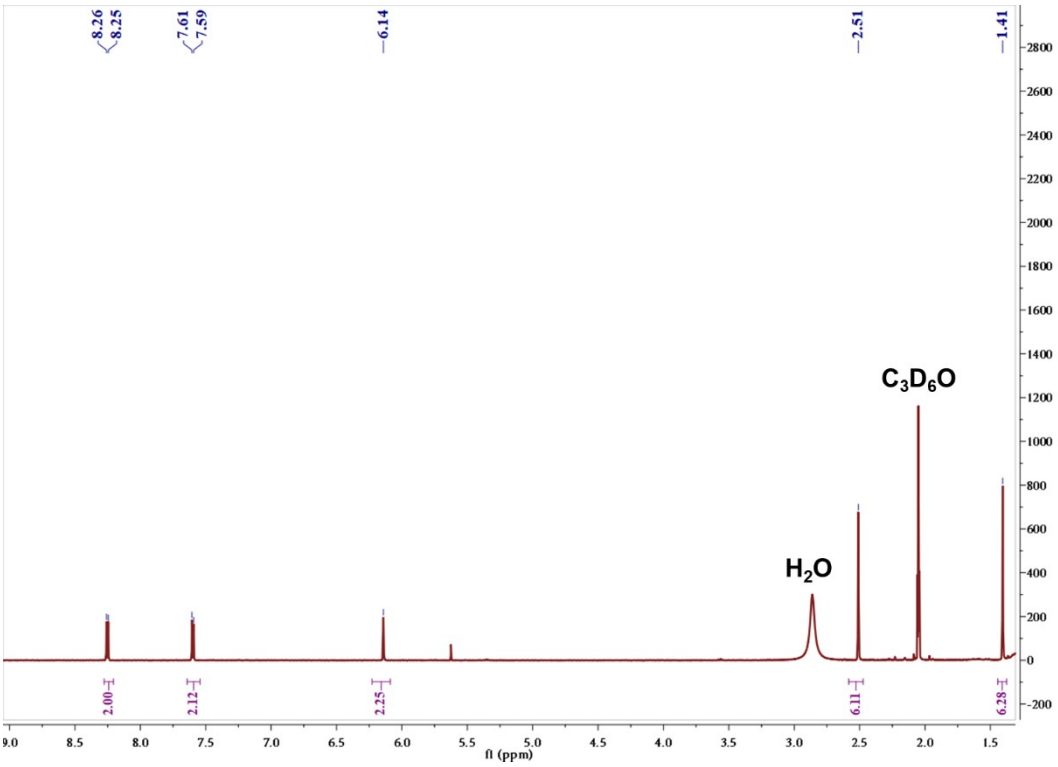


**Figure S1.** The $^{1}H$ NMR plot of BET.

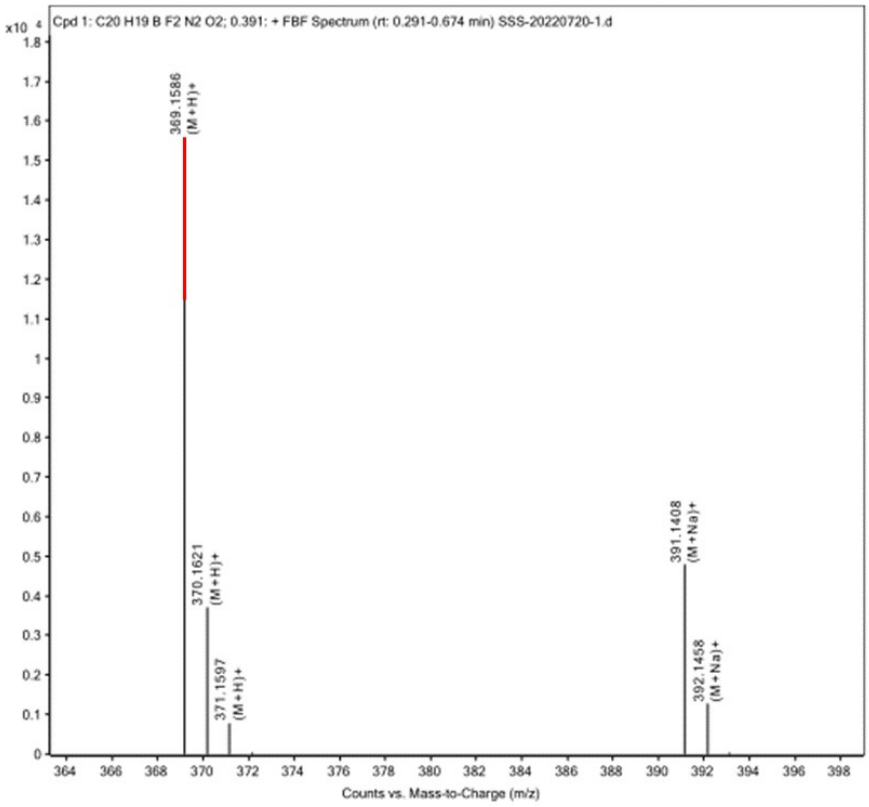


**Figure S2.** The LC/MS plot of BET.

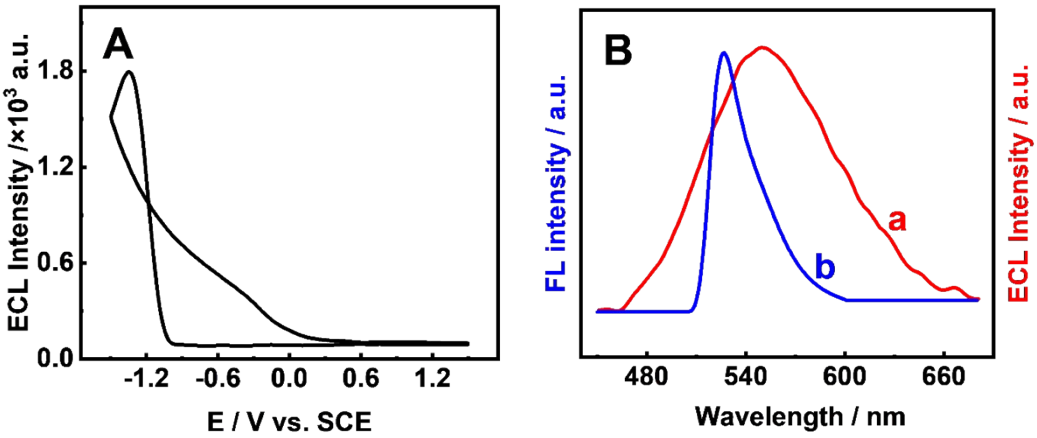


**Figure S3.** (A) The ECL plot of BET acquired with 2 mM p-benzoquinone. (B) The corresponding ECL plot (curve a) and FL spectrum (curve b) of BET.

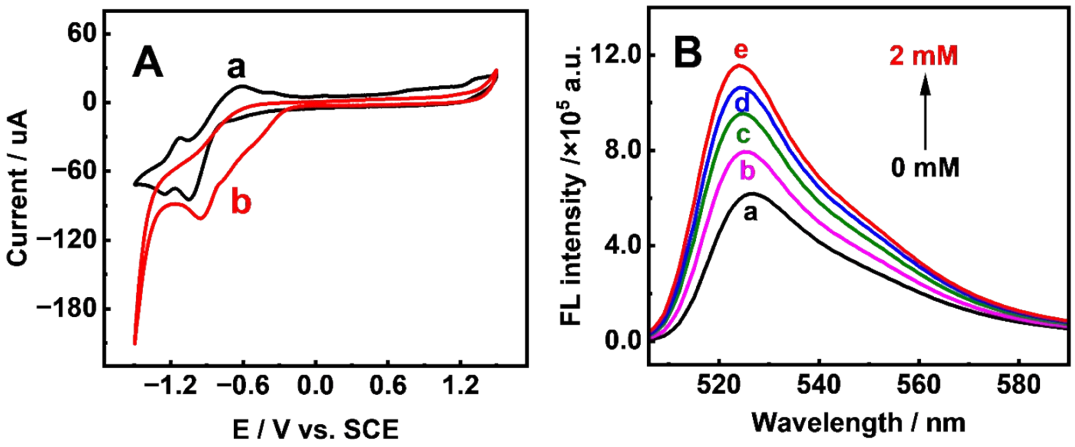


**Figure S4.** The (A) CV plots of BET (curve a) and BET + 2 mM acetic acid (curve b). The (B) FL spectra of BET (curve a) and BET + acetic acid (0.5-2.0 mM, curves b-e).

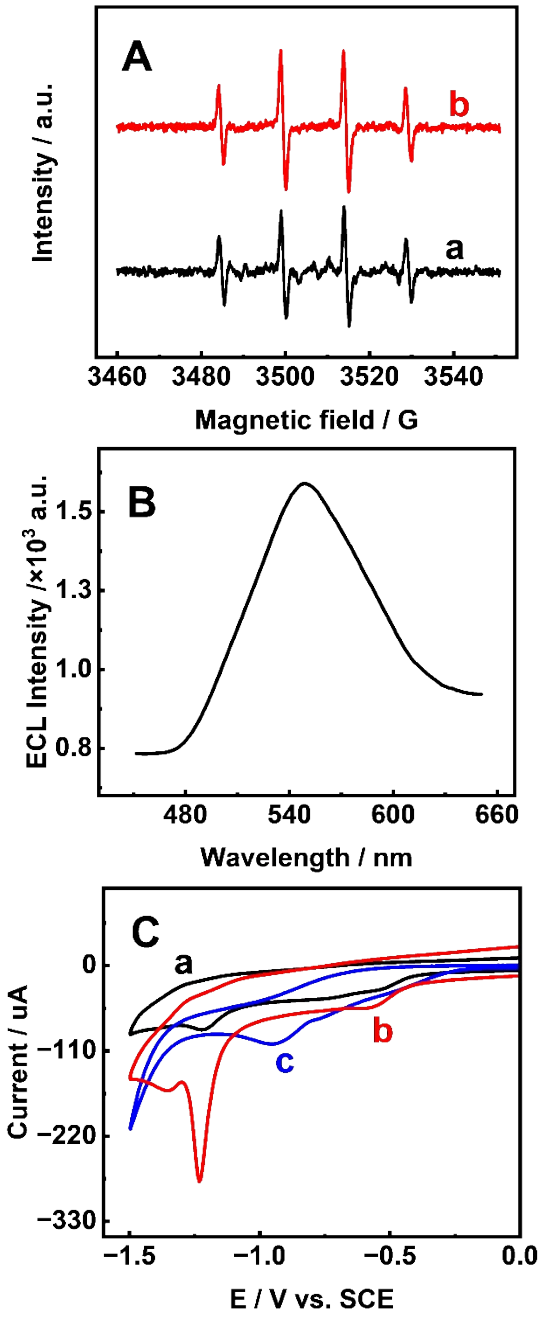


**Figure S5.** (A) The EPR plots recorded in the 2 mM $K_2S_2O_8$ solution without (curve a) and with acetic acid (curve b). (B) The ECL spectrum of the BET/GCE + 2 mM $K_2S_2O_8$. (C) The CV plots of the BET/GCE (curve a), BET/Pd@MOFs/GCE (curve b) and BET/Pd@MOFs/GCE + 10 mM $Cu^{2+}$ (curve c) acquired in the PBS with 2 mM $K_2S_2O_8$.

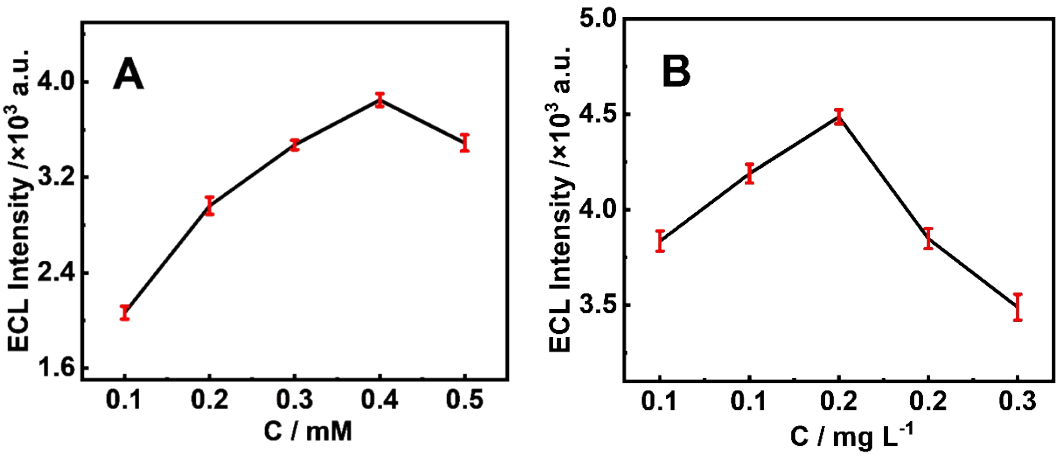


**Figure S6.** The influences of the concentrations of the BET (A) and Pd@MOFs (B) on the ECL signals.

**Table S1.** Comparison of the analytical performances of different $Cu^{2+}$ detection assays.

| Method | Linear Range | LOD | Reference |
|---|---|---|---|
| FL | 0.10 μM–5.00 μM | 5.61 nM | [1] |
| EC | 50.00 nM–12.00 μM | 13.00 nM | [2] |
| PEC | 1.00 nM–10.0 μM | 0.40 nM | [3] |
| ECL | 0.20 nM–1.00 μM | 0.07 nM | [4] |
| ECL | 1.0 pM–500.0 nM | 0.33 pM | [5] |
| **ECL** | **1.0 pM-100.0 pM** | **0.12 pM** | **This work** |

| Sample | Added (pM) | Found (pM) | Recovery (%) | RSD (%) |
|---|---|---|---|---|
| Lake water | 1.0 | 1.03 1.02 1.02 | 102.4 | 0.53 |
| | 10.0 | 9.93 9.98 10.02 | 99.8 | 4.08 |
| | 100.0 | 100.2 100.0 100.1 | 100.1 | 1.97 |

**Table S2.** Detection of $Cu^{2+}$ in the Chuyang lake water sample.

**References**


1. J. Hou, P. Jia, K. Yang, T. Bu, S. Zhao, L. Li and L. Wang, *ACS Appl. Mater. Interfaces*, 2022, **14**, 13848−13857.
2. F. F. Wang, C. Liu, J. Yang, H. L. Xu, W. Y. Pei and J. F. Ma, *Chem. Eng. J.*, 2022, **438**, 135639.
3. J. Li, F. Mo, L. Guo, J. Huang, Z. Lu, Q. Xu and H. Li, *Sens. Actuators B Chem.*, 2020, **328**, 129032.
4. J. Chen, Q. Wang, X. Liu, X. Chen, L. Wang and W. Yang, *Chem. Commun.*, 2020, **56**, 4680-4683.
5. Q. Han, C. Wang, Z. Li, J. Wu, P. K. Liu, F. Mo and Y. Fu, *Anal. Chem.*, 2020, , **92**, 3324−3331.